

Nonvolcanic tremor along the Oaxaca segment of the Middle America subduction zone

Michael R. Brudzinski,¹ Héctor R. Hinojosa-Prieto,¹ Kristen M. Schlanser,¹ Enrique Cabral-Cano,² Alejandra Arciniega-Ceballos,³ Oscar Diaz-Molina,² and Charles DeMets⁴

Received 1 September 2008; revised 13 January 2010; accepted 6 April 2010; published 19 August 2010.

[1] The Oaxaca subduction zone is an ideal area for detailed studies of plate boundary deformation as rapid convergent rates, shallow subduction, and short trench-to-coast distances bring the thermally defined seismogenic and transition zones of the plate interface over 100 km inland. Previous analysis of slow slip events in southern Mexico suggests that they may represent motion in the transition zone, defining the downdip edge of future megathrust earthquakes. A new deployment consisting of broadband seismometers distributed inland along the Oaxaca segment provide the means to examine whether nonvolcanic tremor (NVT) signals can also be used to characterize the boundary between the seismogenic and transition zones. In this study, we established that NVT exists in the Oaxaca region based on waxing and waning of seismic energy on filtered day-long seismograms that were correlated across neighboring stations and were further supported by appropriate relative time moveouts in record sections and spectrograms with narrow frequency bands. Eighteen prominent NVT episodes that lasted upwards of a week were identified during the 15 months analyzed (June 2006 to September 2007), recurring as frequently as every 2–3 months in a given region. We analyze NVT envelope waveforms with a semiautomated process for identifying prominent energy bursts, and analyst-refined relative arrival times are inverted for source locations. NVT burst epicenters primarily occur between the 40–50 km contours for depth of the plate interface, except in eastern Oaxaca where they shift toward the 30 km contour as the slab steepens. NVT hypocenters correlate well with a high conductivity zone that is interpreted to be due to slab fluids. NVT is more frequent, shorter in duration, and located further inland than GPS-detected slow slip, while the latter is associated with a zone of ultra-slow velocity interpreted to represent high pore fluid pressure. This zone of slow slip corresponds to approximately 350°C–450°C, with megathrust earthquakes, microseismicity, and strong long-term coupling occurring immediately updip from it. This leaves NVT primarily in a region further inland from the thermally defined transition zone, suggesting that transition from locking to free slip may occur in more than one phase.

Citation: Brudzinski, M. R., H. R. Hinojosa-Prieto, K. M. Schlanser, E. Cabral-Cano, A. Arciniega-Ceballos, O. Diaz-Molina, and C. DeMets (2010), Nonvolcanic tremor along the Oaxaca segment of the Middle America subduction zone, *J. Geophys. Res.*, 115, B00A23, doi:10.1029/2008JB006061.

1. Introduction

[2] Subduction zones are where oceanic lithosphere is recycled into Earth's interior [Stern, 2002], and where the largest, devastating megathrust earthquakes rupture when plate motion accumulates tectonic stresses on the locked, seismogenic zone of the plate interface. Moving downdip along the plate interface, from this cold and brittle zone, the increasing pressures, temperatures, and slab dehydration/metamorphic reactions generate a transition in frictional behavior from stick slip to stable sliding [e.g., Hyndman and Wang, 1993; Scholz, 1990]. Recent observations have now revealed slow slip episodes (SSE) that occur regularly in this

¹Department of Geology, Miami University of Ohio, Oxford, Ohio, USA.

²Departamento de Geomagnetismo y Exploración, Instituto de Geofísica, Universidad Nacional Autónoma de México, Mexico City, Mexico.

³Departamento de Vulcanología, Instituto de Geofísica, Universidad Nacional Autónoma de México, Mexico City, Mexico.

⁴Department of Geology and Geophysics, University of Wisconsin-Madison, Madison, Wisconsin, USA.

deeper transitional zone with motion indicating release of accumulated strain [Dragert *et al.*, 2001; Lowry *et al.*, 2001; Ozawa *et al.*, 2002]. The duration of these episodes is much greater than earthquakes, yet they are accompanied by low-level seismic vibrations (nonvolcanic tremor, NVT) [Obara, 2002; Rogers and Dragert, 2003; Szeliga *et al.*, 2004]. While this episodic tremor and slip (ETS) has been proposed to impact the likelihood of megathrust earthquakes [Mazzotti and Adams, 2004; Hirn and Laigle, 2004; Kodaira *et al.*, 2004], processes that govern ETS and potential relationships to major earthquakes remain unknown.

[3] NVT was discovered in Nankai subduction zone, and was originally interpreted as hydraulic fracturing due to subducting oceanic slab dehydration/metamorphic reactions [Obara, 2002; Katsumata and Kamaya, 2003]. Subsequently, NVT has been observed in other subduction zones including Cascadia, Alaska, Costa Rica [Schwartz and Rokosky, 2007], the Guerrero area of Mexico [Payero *et al.*, 2008]; and even in the dextral strike-slip San Andreas fault [Nadeau and Dolenc, 2005]. Compared to ordinary earthquakes, subduction zone NVT activity is not easily detectable or located with traditional earthquake routines. This is mainly due to their weak, emergent waveforms that obscure arrival times, and limited frequency range of 1 to 10 Hz that may be overprinted by local microseismicity. NVT signals persist for longer durations than earthquakes, varying from minutes to several days, but they do contain bursts of energy lasting a few seconds that are best seen in horizontal components and have moveouts consistent with S wave phase arrivals. When recorded clearly by a dense network in Japan, stacking of similar NVT seismograms have revealed *P* wave energy as well [Shelly *et al.*, 2006]. Detailed analysis of NVT in Japan indicates they occur at the plate interface and have thrust mechanisms, suggesting that shear faulting is an alternative hypothesis for the origin of NVT [Ide *et al.*, 2007b; Shelly *et al.*, 2007].

[4] Our study focuses on the Middle American subduction zone, which has frequent great earthquakes close to large cities such as the 1985 Michoacán earthquake that caused 10,000 casualties and billions of dollars of damage [e.g., Beck and Hall, 1986]. The Oaxaca segment offers an ideal opportunity for detailed studies of ETS and megathrust seismicity due to its relatively rapid convergent rates, unusually shallow subduction angle, and short megathrust earthquake recurrence intervals (decades) [Anderson, 1989; Kostoglodov and Ponce, 1994]. In particular, the ~50 km trench-to-coast distances bring the seismogenic and transitional zones of the plate interface greater than 100 km inland, such that in depth geophysical studies are possible within coastal Oaxaca (Figure 1). Continuous GPS recording in Oaxaca that began 14 years ago [e.g., Márquez-Azúa and DeMets, 2003], constituting the longest continuous GPS record in southern Mexico, defines ten distinct episodes of transient slip from 1993 to 2007 [Brudzinski *et al.*, 2007; Correa-Mora *et al.*, 2008, 2009]. Considering the correlation between slow slip events and NVT elsewhere [e.g., Rogers and Dragert, 2003], we designed a joint seismic GPS array in and around the Oaxaca state to determine whether slow slip events are accompanied by tremor and/or microseismicity, and if so, what the patterns are in space and time.

[5] In this study, we establish that episodic NVT signals similar to other subduction zones occur in Oaxaca. We then

proceed to investigate the spatial and temporal distribution of NVT within the state of Oaxaca, including the duration, recurrence, and along-strike distribution of NVT episodes. Finally, we discuss NVT source locations in the context of other observed phenomenon, including megathrust earthquakes, microseismicity, slow slip events, ultraslow velocity zones and high conductivity zones.

2. Existence of Nonvolcanic Tremor in Oaxaca

[6] The new joint seismic GPS network includes seven portable Guralp CMG-3T three-component broadband seismometers installed in the summer of 2006. The broad network was specifically designed to detect and monitor NVT and microseismicity signals along the Oaxaca segment (Figure 1). The seismic stations are distributed inland over an area of ~300 km east-west and 200 km north-south with nominal ~80 km station spacing, and pockets of higher density GPS instrumentation [Brudzinski *et al.*, 2007; Correa-Mora *et al.*, 2008, 2009]. This study examines the first ~15 months of seismic recording from June 2006 to September 2007. We do not discuss data from the northwestern station OXBV in detail as we found it was far enough away from the remaining stations that it typically only showed signals consistent with the rest of the network during larger earthquakes. The remainder of the network was used to characterize whether NVT exists in our network during the 15 month time span.

[7] Our search for NVT began with visual inspection of bandpass (1–5 Hz) filtered day-long waveforms from the network to see whether there were coherent changes in amplitude across the network. We found many cases where the amplitudes waxed and waned coherently at neighboring stations for several days (Figure 2). The emergent nature and long durations of the apparent NVT signals clearly distinguish them from earthquakes [e.g., Obara, 2002], where earthquakes appear as thin vertical bars in day-long seismograms. The coherent changes in amplitude between neighboring stations over minute-to-hour time scales indicate they are not due to cultural noise local to a given site which would be variable from station to station on those time scales. The fact that not all network sites show the raised amplitudes during a given episode and that they appear strongest on inland stations further indicates they are more likely due to NVT than weather-related noise. The latter issue was also addressed by confirming that storms are not responsible for any of the apparent NVT episodes documented in this study (<http://www.solar.ifa.hawaii.edu/Tropical/Data/>). Instead, Figure 2 shows 8 examples of days with increased activity in the tremor passband throughout the 15 months of recording.

[8] We next examine bursts of energy within the time periods of raised amplitudes to see whether they are consistent with a coherent nonearthquake source. These bursts of energy have typical durations of 10 s, and the filtered envelope seismograms show relative arrival times between stations with an expected moveout pattern for events within our network (Figure 3). These moveouts are the primary information used to investigate source locations in section 4.

We also produced spectrograms for the bursts of energy to confirm that the signals are primarily restricted to the 1–10 Hz passband expected for NVT (Figure 3) [e.g., Obara,

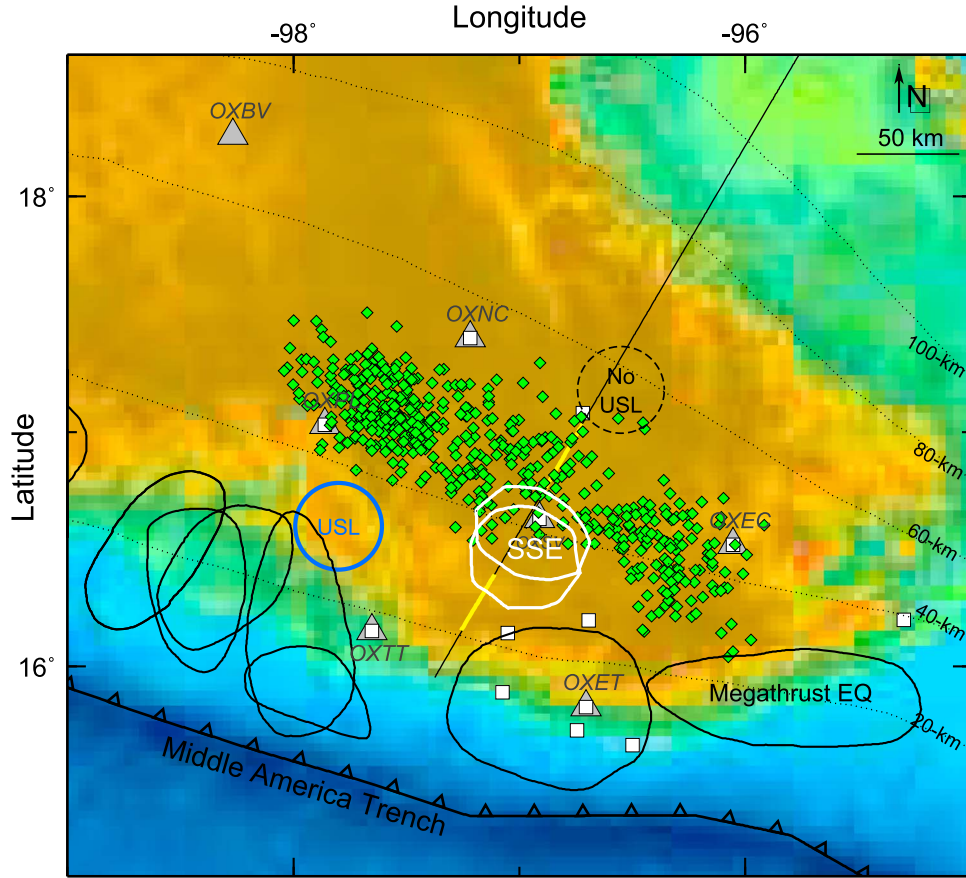


Figure 1. Map of the study region focused along the Oaxaca segment of the Middle American subduction zone. Grey triangles (seismic) and white squares (GPS) show the state of the joint network in 2006–2007 that is used to determine the extent of nonvolcanic tremor in July 2006 (green line, this study) and the 100 mm slip contour for slow slip events in early 2006 and early 2007 (white ovals) [Correa-Mora *et al.*, 2008, 2009]. Black ovals are approximate rupture zones of large subduction thrust earthquakes over the past 50 years as estimated from locations of rupture aftershocks [e.g., Astiz and Kanamori, 1984; Courboulex *et al.*, 1997; Singh *et al.*, 1980, 1997; Stewart *et al.*, 1981; Tajima and McNally, 1983]. Straight line is a profile of magnetotelluric measurements with areas of high conductivity near the subduction interface highlighted in yellow [Jödicke *et al.*, 2006]. Dotted lines are isodepths of the subducting plate from analysis of seismicity [Pardo and Suarez, 1995]. Blue circle indicates where an ultra-slow velocity layer has been detected, and dashed circle indicates where it is absent. Colored background illustrates elevation and bathymetry.

2002], whereas local earthquakes typically have prominent energy above 10 Hz. This last comparison is important because microseismicity is common in this region, so it was checked on a regular basis to confirm the authenticity of NVT signals.

[9] To further illustrate the different frequency content of the tremor signals relative to local earthquakes and background noise, we follow the approach of previous researchers to calculate the amplitude spectra of each type of signal recorded in our data [Kao *et al.*, 2006; Shelly *et al.*, 2007]. To ensure frequency spectra are representative of source characteristics with minimal path effects, we only analyze seismograms with high signal-to-noise ratios recorded within 50 km of the earthquake or tremor epicenter. For each seismogram, the signal segment is taken from 1 s before to 9 s after the arrival of the largest amplitude (a total of 10 s), whereas the background noise is taken from a relatively quiet portion away from the signal

segment. To make a more meaningful comparison between tremors and earthquakes with different magnitudes, we normalize both the signal and noise spectra against the amplitude of background noise at 1 Hz at each station. Finally, frequency spectra of all seismograms from the same type of signal are stacked by taking the median value at each frequency to give typical spectrum curves (Figure 4). Tremor spectra are from all episodes analyzed in section 4, while seismograms of local earthquakes are sorted by magnitude as determined by a preliminary study of local seismicity within the network [Jensen *et al.*, 2008]. In general, the tremor frequency spectra show relatively large amplitudes in the frequency range of 1–5 Hz with a rapid falloff at higher frequencies (5–20 Hz). At 1 Hz and below, the amplitudes of tremor spectra are comparable to those of earthquakes with $M_L \sim 1$ and background noise. For higher frequencies, however, even small earthquakes are able to excite much more high frequency content than tremor

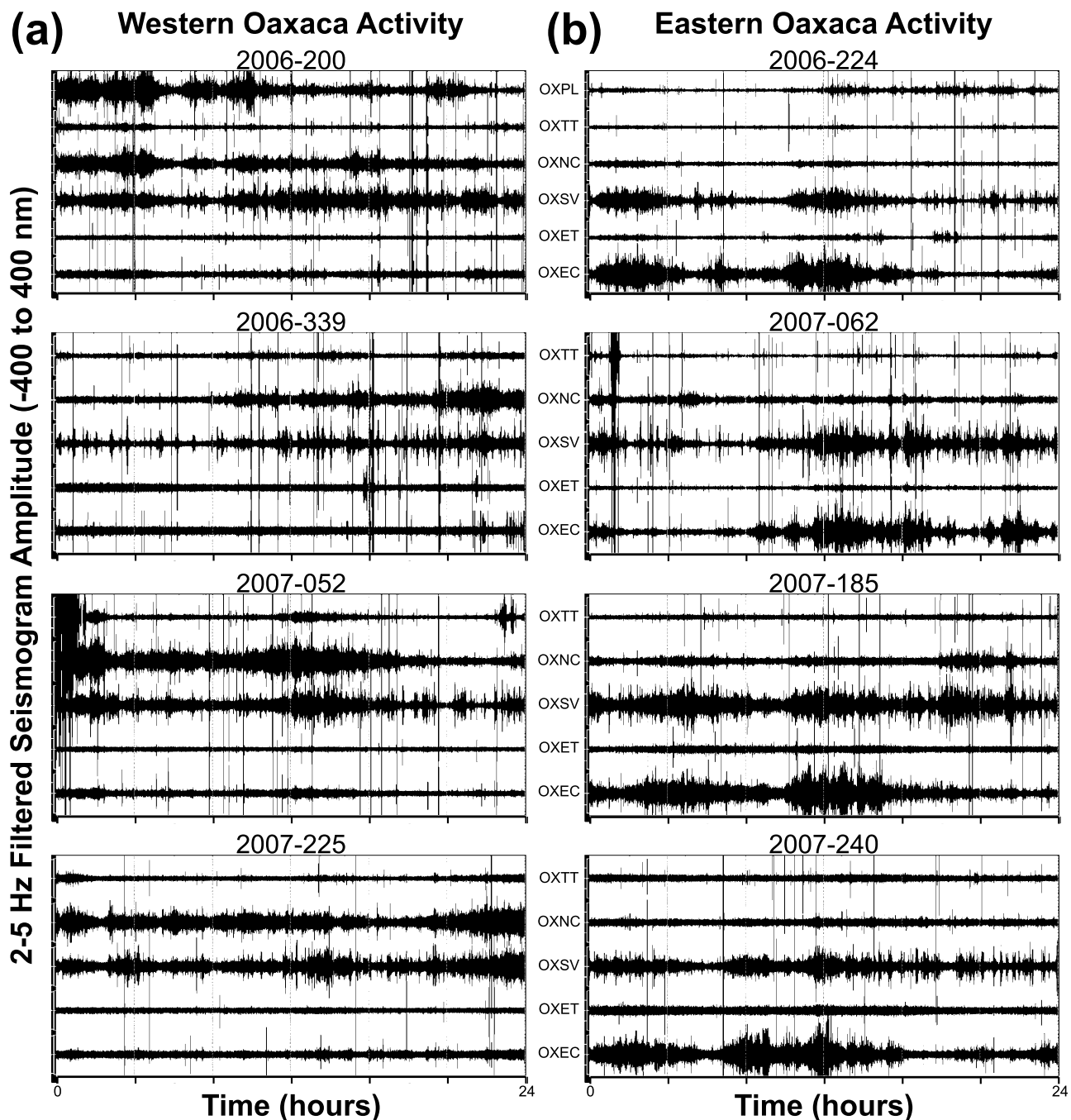


Figure 2. Example seismograms during prominent NVT episodes in the (a) western and (b) eastern ends of the seismic network. Day-long filtered horizontal component seismograms are ordered from west to east, with OXPL only available for days 2006-200 and 2006-224. They show correlated waxing and waning of energy on the western inland stations (Figure 2a) and similar evidence on eastern inland station stations (Figure 2b). These seismograms are an expanded view of the peaks in the mean amplitude time series shown in Figure 4, at OXNC and OXEC, respectively. For all seismograms, amplitude scale is -400 to 400 nm.

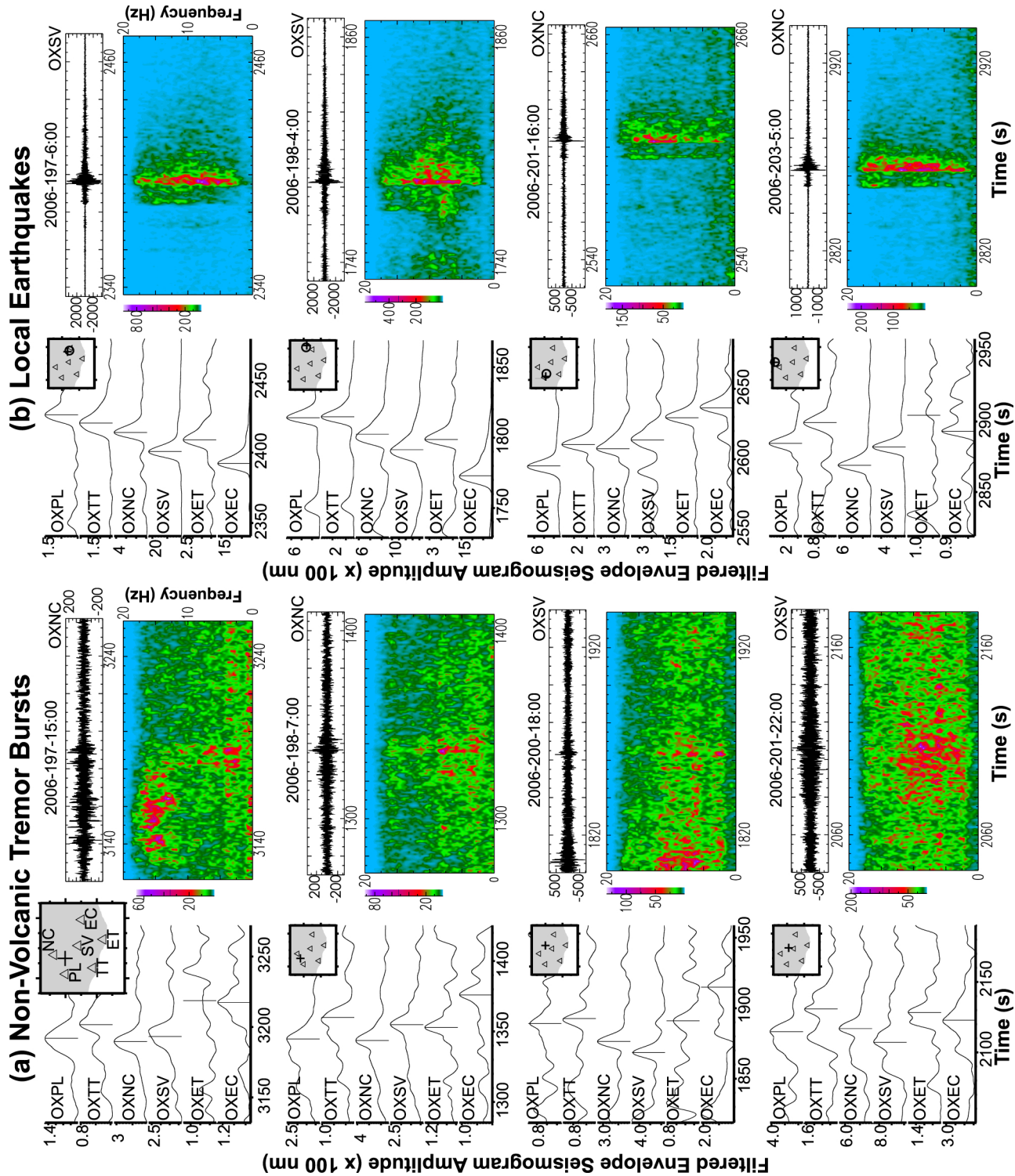


Figure 3

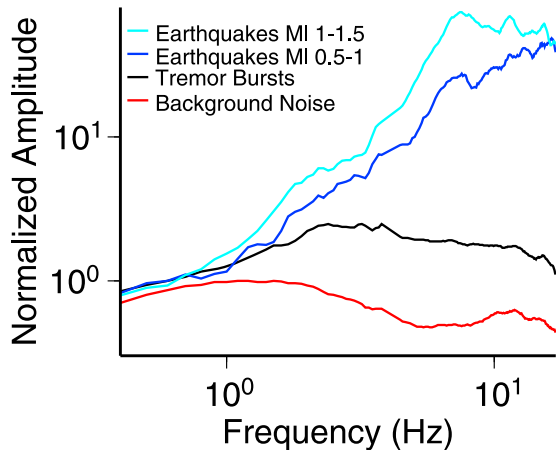


Figure 4. Comparison of frequency spectra between non-volcanic tremor, local earthquakes, and background noise in the Oaxaca seismic network. All waveforms are calibrated to the same short-period velocity sensor and gain range before spectra are calculated. Tremor spectra differ markedly from local earthquakes at frequencies higher than 5 Hz, even when amplitudes are similar amplitudes near 1 Hz.

sources. This contrast in frequency characteristics has led many to suggest tremor and earthquakes are fundamentally different source processes.

3. Prevalence of Nonvolcanic Tremor in Oaxaca

[10] To quantitatively investigate when NVT is occurring in our network over the full 15 month time span, we utilize an automated NVT scanning method [Brudzinski and Allen, 2007]. This technique begins by removing the instrument response and applying a filter with a passband of 1–6 Hz. Next, it takes the absolute value and calculates the envelope, before finding the mean amplitude of the whole hour-long time series. Since various nontectonic factors can influence the amplitude, we limit our analysis to hours when culture-generated noise is at a minimum and exclude hours during which signals from known, large earthquakes or other spikes, such as those used for instrument calibration, are present. To help reduce longer-term noise trends that can exist at a few stations, we high-pass filter the entire mean amplitude time series to signals with periods less than about a week. Last, we average amplitudes over a four-day moving window to help accentuate sustained tremor activity. It is typical to normalize values in this last step, but since all of the instruments in this network are identical, we preserve the actual amplitude values to help illustrate relative amplitude differences between peak activity at inland stations OXPL, OXNC, and OXEC versus those at coastal stations OXTT and OXET.

Figure 3. Example waveforms, location maps, and spectrograms for four (a) NVT bursts and (b) earthquakes. For each event, Figure 3a shows smoothed envelope waveforms (curves) for stations from west to east (curves), with phase pick marked by the vertical line. Small map inset shows stations (triangles) and epicenters (crosses for our method, circles for earthquakes from Jensen et al. [2008]). Figure 3b shows a 1–20 Hz filtered seismogram from (top) a station near the epicenter and (bottom) its corresponding spectrogram.

[11] In the final time series, large peaks suggest periods during which NVT dominates the seismic recordings (Figure 5). We find 12 time periods when peaks rise above background noise in the mean amplitude time series at greater than 99% confidence interval during the 15 months analyzed (5 at OXNC, OXTT or OXPL; 1 at OXS; 6 at OXEC). There are also 6 different time periods when peaks exceed the 95% threshold (3 at OXNC, 1 at OXS, and 2 at OXEC).

We were able to confirm NVT in each case by inspecting individual seismograms and corresponding spectrograms. For example, Figure 2 shows how stations have large seismogram amplitudes over the course of a day during each of the 4 largest peaks in the OXEC mean amplitude time series (Figure 2a) and during 4 peaks in the OXNC time series (Figure 2b).

4. Location of Nonvolcanic Tremor in Oaxaca

[12] For our analysis of NVT source locations, we begin by investigating all 18 time periods that exceeded either the 99% or 95% threshold in the mean amplitude time series. For each episode, we attempt to determine locations of bursts of activity during the nighttime hours with the largest mean amplitudes, presumably when tremor is most active and clearly defined. We then examine tremor activity on a daily basis during a 5 month time period spanning the slow slip events to see whether tremor locations can be obtained at times outside the prominent episodes. Following these broader searches, we focus on the best recorded episode of NVT in July 2006 to examine the hypocentral patterns of the best constrained locations for a single episode (Figure 2). This episode was selected in part due to the lack of data recording at western station OXPL after September 2006 and at central station OXS from mid-March to mid-May 2007.

4.1. Source Location Approach

[13] We developed a semiautomated algorithm for finding individual bursts during hours with large mean amplitudes in the NVT passband, and use relative arrival times across our network to determine the source locations. This process begins the same way as the mean amplitude scanning algorithm that removes the instrument response from an hour-long seismogram, bandpass filters at 1–6 Hz, takes the absolute value and calculates envelope seismograms. Considering the similarity in processing, it was natural to focus our attention on hours with large mean amplitudes. To help clarify the bursts of energy in a given hour from station to station, we smooth the envelopes with a 0.06 low-pass filter and stack the three components to enhance NVT signals with respect to background noise. We initially attempted our analysis using single horizontal component seismograms, but found for a given event that the most prominent *S* wave arrivals occurred on different components depending on the station back-azimuth and incidence angle. Stacking the components together gave a more reliable recording of the

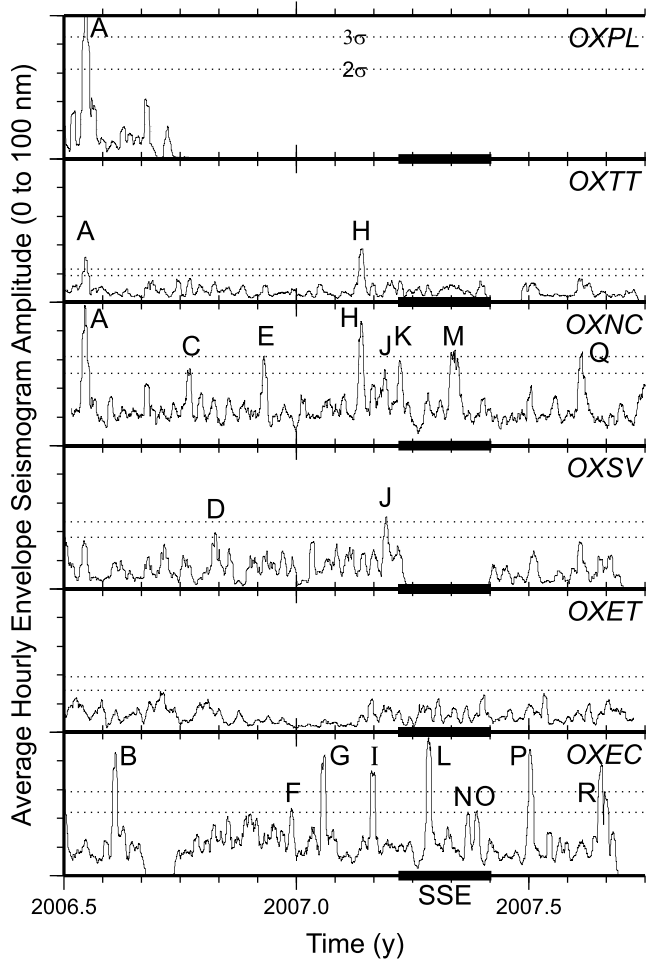


Figure 5. Evidence for the prevalence of NVT episodes in the seismic network during the first 15 months of recording. Smoothed time series of hourly mean amplitudes in the NVT passband are shown for all six stations used in this study, ordered from west to east. Dotted lines show the 2σ and 3σ variations from the average value for the smoothed time series and represent time periods when seismic signals rise above background noise at greater than 95% and 99% confidence interval, respectively. Peaks rising above the 2σ line are labeled and correspond to labels in Figures 6 and 7. Peaks are times when the NVT passband is most active and suggest NVT is prominent near those stations.

tremor signal, as opposed to simply reducing the noise. For each waveform used to determine our best events discussed below, the average signal-to-noise ratio for the stacked components are 3.5, whereas the average for any individual component was no larger than 2.6.

[14] To identify when signals are most active across our network, we examine a stack of all the station time series together. We use STA/LTA ratios greater than 2 (time windows are 10/100) to target distinct prominent pulses rising above background noise in this network activity time series. For each peak time, we examine envelope waveforms around that time for stations that have signal-to-noise ratios of at least 1.5. For cases with coherent signals and reasonable moveouts, we select the peak times that best represent

the station-to-station relative timing of energy packets and treat them as S wave arrival times. This approach is dictated by the emergent nature of NVT and small signal-to-noise ratios, but we estimate that the median picking uncertainty is less than 1 s based on evaluation of over 100 waveforms.

[15] Previous NVT studies have commonly relied on higher station coverage to utilize automated cross-correlation routines to scan for NVT source locations within vast data sets [Kao and Shan, 2004; Obara, 2002; Wech and Creager, 2008]. The prevalence of local earthquakes inhibits an automated determination of NVT source locations in Oaxaca, as particular scrutiny of spectrograms is needed to discriminate between bursts of NVT and small local earthquakes. As one might expect, we find it is far more common for earthquakes to be identified with this STA/LTA selection routine than in Cascadia [Boyko and Brudzinski, 2010], such that care is needed to separate these cases from that of tremor. Moreover, the limited density of stations requires that seismograms are examined in detail to verify source locations are derived from clear, coherent NVT signals. In fact, attempts to refine the pick times using cross-correlation of the envelope seismograms result in location errors approximately a factor of 2 larger than when we visually refine peak times. We suggest this is due to the relatively large station spacing (~ 80 km) compared with previous studies, which results in more variable envelope waveforms from station to station, but we cannot rule out that our phase picking approach is subjective and underestimates location errors by up to a factor of 2.

[16] When a coherent NVT burst is observed at a minimum of four stations (five for the focused analysis of the July 2006 episode), the analyst-refined arrival times are used to invert for a source location using a 1D regional S wave velocity model that accounts for the presence of rocks from the Acatlan metamorphic complex of the Oaxaca region [Valdes et al., 1986]. The source inversion is performed using the computationally efficient ELOCATE algorithm [Hermann, 2004], which also produces nominal uncertainties based on incoherence between arrival times. We also recalculated locations many times by randomly adjusting arrival times between -1.0 and 1.0 s to estimate the location uncertainty potentially due to picking error, finding the locations differed on average 3 km in the horizontal direction and 10 km in the vertical direction. In addition, we obtained formal location uncertainty estimates based on bootstrap location reliability [Efron, 1979; Wech and Creager, 2008]. For each event we iteratively remove each station from the input arrival times, one at a time, and search for a location. We interpret the median of the resulting cloud of locations as the source centroid epicenter with an error estimated by the median absolute deviation. We tested this scheme against the wave trains of 15 local earthquakes during the July 2006 episode that were detected and located with our semiautomated technique. Despite the fact that many of the events occurred at the edge of our network, this test found that two-thirds of the earthquake locations from our method lay within 15 km of the epicenters determined with the Antelope Software package [Jensen et al., 2008], with a median epicentral difference of 13 km. To help focus on our best resolved locations in our discussion of patterns in NVT source locations, we only interpret the events with all forms of uncertainty less than

15 km in the horizontal and vertical directions. Plots of envelope waveforms and resulting source location maps for each of the NVT events for the July 2006 episode and the 15 local test earthquakes can be found in the auxiliary material.¹

4.2. Spatial and Temporal Distribution of Tremor Sources in Oaxaca

[17] We have successfully determined tremor source locations using the semiautomated processing technique for each of the 18 prominent episodes identified in mean amplitude processing. The epicentral distributions indicate that the tremor source region hops back and forth along strike over time (Figure 6), focusing around the 40 km contour of the plate interface. Most episodes analyzed in this study last for ~3 days and result in a distribution of epicenters about 50 km wide. A few episodes that last upwards of a week result in larger distributions of ~120 km width (Figures 6a and 6p). Although these measurements linking source area to duration are limited, these results appear to be consistent with previous results in other regions that find the moment associated with ETS is proportional to duration [e.g., Ide *et al.*, 2007a].

[18] We next examine the along-strike distribution of tremor source locations in time (Figure 7). The source locations obtained for the different episodes displays a complicated pattern that is difficult to generalize. Figure 7 helps to illustrate that the central part of the network appears to have been slightly more active around the time of the slow slip event. We also find there are five episodes of similar along-strike extent west of 97.4°W and seven episodes of similar along-strike extent east of 96.6°W. Based on the similarity of episodes in these two regions, we calculate an approximate recurrence interval to be ~2 months in the eastern region, and ~3 months in the western region, although it is still possible that the slight differences in location from episode to episode indicate that the patch of tremor activity may not be identical each time. Autocorrelation analysis to search for low-frequency earthquakes and subsequent cross-correlation of similar waveforms to refine source locations may be able to further address this, but the broad station spacing could make that analysis difficult.

[19] The frequent recurrence of tremor episodes in Oaxaca is surprising considering it has not previously been observed in the neighboring Guerrero segment or in Cascadia, another warm subduction zone. However, short NVT episode recurrences on the order of 3–6 months have been observed in Nankai [e.g., Obara, 2002; Obara and Hirose, 2006], albeit with a substantially more advanced seismic network [Okada *et al.*, 2004; Obara *et al.*, 2005]. The similarity between Nankai and Mexico is further revealed when one also considers that the short NVT recurrence interval we observe with seismic data is quite different from the 12–24 months recurrence of prominent GPS-detected slow slip events observed in Oaxaca over the past 10 years [Brudzinski *et al.*, 2007; Correa-Mora *et al.*, 2008, 2009], with only slightly larger amounts of NVT activity occurring within the time period of slow slip (Figure 7). In Nankai, so-called short-

term events with prominent NVT recur every 3–6 months without GPS detectable slip [e.g., Obara, 2002; Obara and Hirose, 2006], while a few long-term events with GPS-detected slow slip and without much increase in tremor recurring with frequency on the order of 5 years [e.g., Hirose *et al.*, 1999; Hirose and Obara, 2005; Ozawa *et al.*, 2002; Schwartz and Rokosky, 2007]. The frequent episodes of NVT in Nankai have been linked to small slips only detectable on tiltmeters [e.g., Obara *et al.*, 2004], but there are currently no tiltmeter or strainmeter instruments operating in Oaxaca to confirm that similar small slips are occurring during the frequent NVT episodes we observe.

[20] Detailed source inversions from Nankai have found that short-term events occur primarily downdip from the long-term events. Previous source inversions for GPS-detected slow slip in Oaxaca find that the majority of slip occurs between 25 and 45 km depth on the plate interface (Figure 1). The tremor epicenters we have determined over the 15 months that span one GPS-detected slow slip episode occur further inland and presumably downdip from the source of slow slip. This appears to be another similarity between Oaxaca and Nankai, further suggesting that the frequent tremor episodes we observe represent so-called short-term events and the less frequent GPS-detected slow slip events represent long-term events.

[21] It is interesting to note that in the Oaxaca case, there appears to be a sparse area of tremor locations further inland from the source region of slow slip (Figure 1). Gaps in tremor have been observed in Nankai [e.g., Obara, 2002] and Cascadia [Kao *et al.*, 2009], but there does not appear to be a similar correlation between the gap in tremor and the location of long-term slow slip episodes in those regions. While the gap in tremor on Vancouver Island has been correlated with the location of historic large crustal earthquakes, there does not appear to be any large crustal earthquakes that correlate with the gap in tremor in Oaxaca.

4.3. Scanning for Tremor Sources Between the Prominent Episodes

[22] To examine the possibilities of tremor activity in the times between the prominent episodes analyzed in the previous section, we attempt a daily search to identify and locate tremor bursts over a 5 month time window. For each day from February 2007 to July 2007, we examine the nighttime hour with the largest mean amplitude in the tremor passband to look for signals emerging from the background noise that have coherent moveouts. Whenever reasonable signals are identified, analyst refined relative times are used to find a tremor burst hypocenter, and those additional events that meet our uncertainty criteria are highlighted in Figure 8.

[23] The epicenters from the additional, less prominent tremor sources appear to be focused in a particular region over the 5 month time period, especially when compared to the distribution of prominent tremor sources over that same time period (Figure 8a). The additional events are somewhat distributed in time despite being focused in space (Figure 8b), but they do appear to be more common during the 2.5 month-long slow slip event than the 2.5 months before and after. In addition to this potential temporal correlation, the locations of less prominent tremor sources primarily occur in a region about the same size as the source of slow slip, but shifted to

¹Auxiliary materials are available in the HTML. doi:10.1029/2008JB006061.

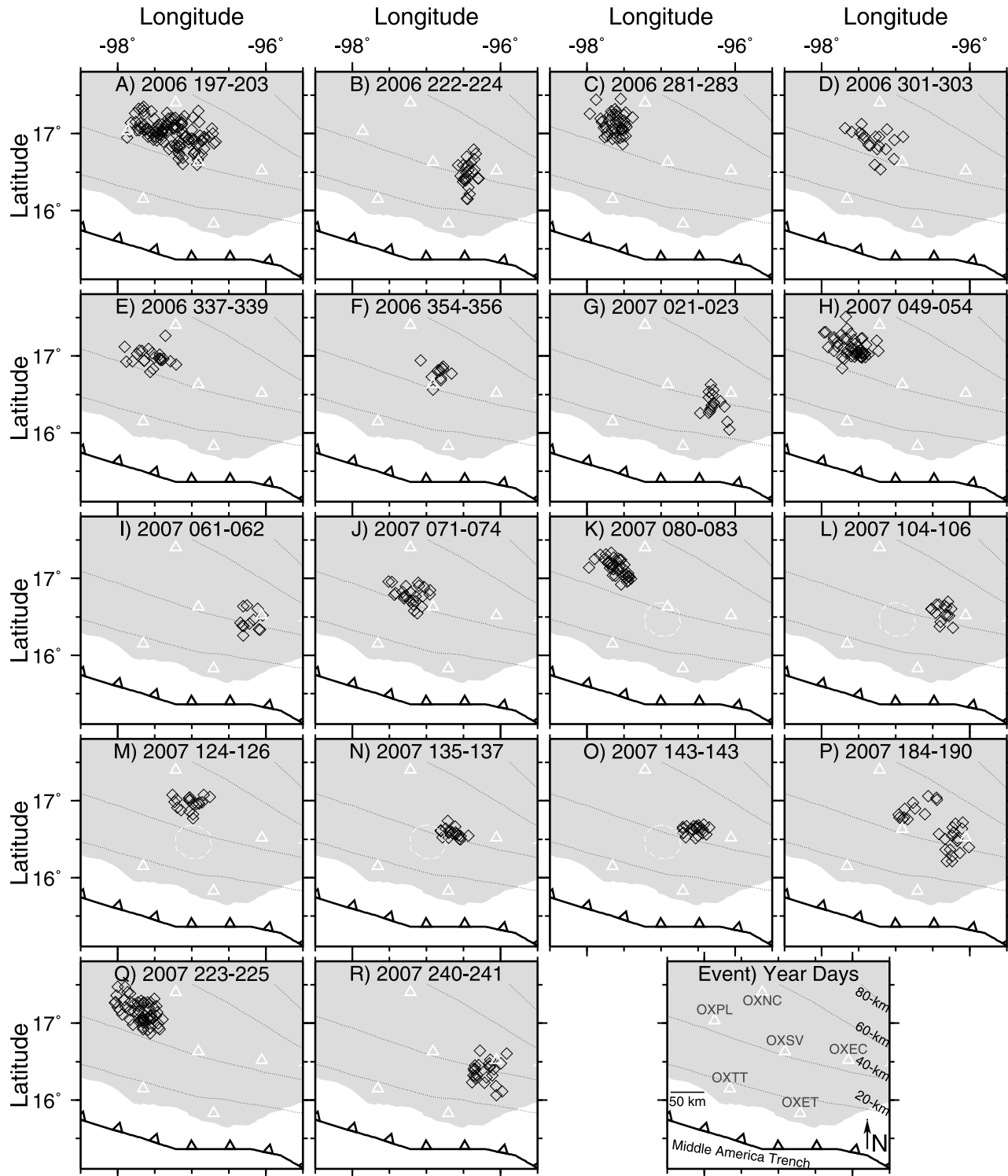


Figure 6. Map showing epicenters of NVT bursts as diamonds for each episode identified in Figure 5. Episodes are labeled with a letter, as well as the year and the days of the year that the episode was prominent. Stations are plotted as triangles when available. White dashed oval indicates source of slow slip when NVT occurs during the GPS-detected slip. Dotted lines are isodepths of the subducting plate from analysis of seismicity [Pardo and Suarez, 1995]. Width of diamonds approximates the median uncertainty in tremor source locations.

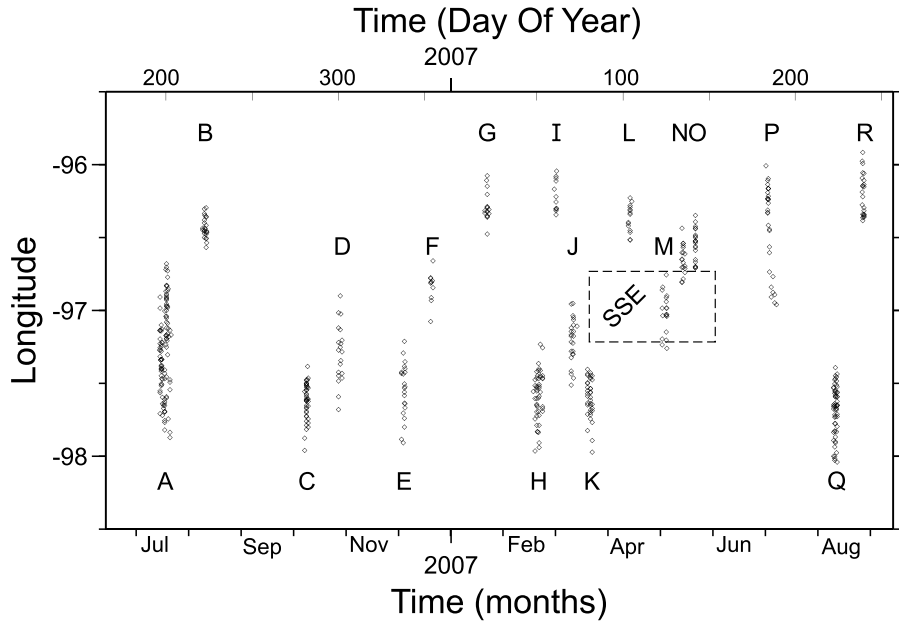


Figure 7. Along-strike locations of NVT versus time, for each episode identified and labeled as in Figures 5 and 6. Dashed box indicates time and along-strike location of GPS-detected slow slip. NVT episodes appear to have some regularity in the along-strike occurrence, and the recurrence of episodes in the eastern and western ends of the network is 2–3 months.

the northeast. In fact, these less prominent sources appear to help fill the area of sparse tremor in the epicenters of prominent tremor (Figure 1).

4.4. Detailed Source Locations of the July 2006 Tremor Episode

[24] To investigate the hypocentral distribution of Oaxaca tremor in further detail, we focus on the source locations of the best recorded episode in July 2006. This episode shows prominent NVT signals at OXPL, OXTT, OXNC, and OXSV on Julian days 197–203 (Figure 3), which also makes it one of the longest episodes during our study period. In this episode, the majority of our source locations are based on timing at these four stations, but we require signals to be picked up on either OXET or OXEC at the far southern and eastern edge of our network to improve our location constraints.

[25] The epicenters of the best resolved NVT bursts in this episode reveal a 125 km long by 75 km wide distribution in the state of Oaxaca between 96°W and 98°W (Figure 9). This patch of NVT activity is centered ~170 km away from the trench, between the 40 km and 60 km contours of the subducting plate [Pardo and Suarez, 1995], and it strikes NW-SE, paralleling the Oaxaca coastline and trench. NVT activity occurs significantly inland from shallow (<35 km) earthquakes and trenchward from a number of deeper (>35 km) earthquakes located with the same network [Jensen et al., 2008] (Figure 9). Both the inland nature of NVT locations and its occurrence in between shallow and deep earthquakes can be demonstrated by comparisons of envelope waveforms of NVT bursts with that of local earthquakes spanning the network during this week of NVT activity (Figure 3). The comparison is particularly useful as the earthquakes in Figure 3 were detected and located with

the same method as that for NVT bursts. Earthquakes near the coast have first arrivals and largest amplitudes on coastal stations OXTT or OXET (third event (Figure 3b)), while waveforms from NVT bursts do not show first arrivals or largest amplitudes on these stations (Figure 3a). Instead NVT waveforms typically show first arrivals and largest amplitudes on stations OXPL and OXSV near the 40 km contour. While NVT often produces similar arrivals and amplitudes on station OXNC near the 60 km contour, it does not show the distinctly earlier arrival time and larger amplitude at OXNC than the most inland deep earthquake creates (fourth event (Figure 3b)). We also find some earthquakes have first arrivals and largest amplitudes on easternmost station OXEC (first and second events (Figure 3b)), but none of the NVT waveforms from the July 2006 episode show this property. Based on these comparisons and taking into account our location uncertainty, we are confident that epicenters of prominent NVT activity during the July 2006 episode are restricted to 130–210 km from the trench (between the 40 and 60 km contours) and only occur in the western part of our network during this episode.

[26] NVT activity is focused during approximately 1 week, between days 197 (July 16) and 203 (July 22) of 2006 (color scale (Figure 9)). There appear to be 2 clusters of NVT activity in space and time. A cluster of events around the beginning of day 198 can be seen from 0 to 40 km distance west of the cross-section line, while another cluster around the beginning of day 201 occurs from 0 to 60 km east of the cross-section line. We can confirm this space-time relationship with envelope waveforms that show western station OXNC typically has the earliest arrival times and largest amplitudes on days 197 and 198 (first 2 events (Figure 3a)), while central station OXSV typically has the earliest arrival

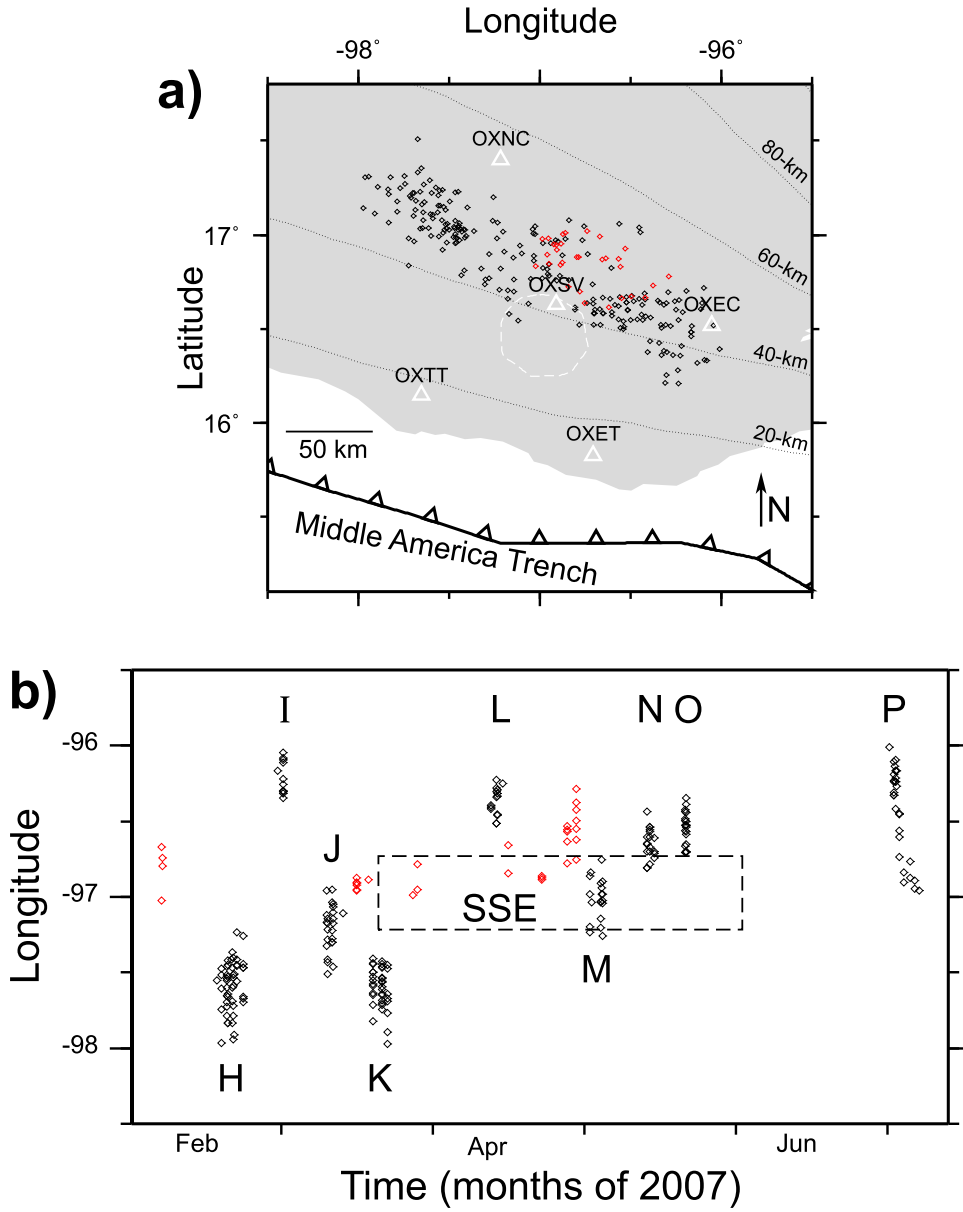


Figure 8. Results of daily examination for tremor sources from February to July 2007. (a) Map of tremor epicenters from daily examination (red), compared with those from the prominent episodes (black) shown in Figure 7. Less prominent tremor sources concentrate to the northeast of slow slip (dashed oval) and fill a sparse area in the distribution of prominent tremor sources. Dotted lines are isodepths of the subducting plate from analysis of seismicity [Pardo and Suarez, 1995]. (b) Along-strike distribution of tremor sources using the symbols from Figure 8a and the layout of Figure 7. Less prominent tremor appears to be more prevalent during the 2.5 month slow slip event than the 2.5 months before and after.

times and largest amplitudes on days 200 and 201 (next 2 events (Figure 3a)). In addition to these 2 primary clusters, we also see evidence for events shifting slightly westward from day 197 to 199 based on arrival times of OXSV becoming later relative to OXNC, which is the opposite direction one would expect if events gradually migrated from one cluster toward the other. This apparent jumping in NVT source locations over a region of previous activity has been documented in Cascadia and Nankai [e.g., Kao *et al.*, 2006; Shelly *et al.*, 2007].

[27] The depths of individual NVT burst hypocenters are illustrated in cross-section A-A' (Figure 10). Depths range from 27 to 54 km, with a median depth of 41 km and median combined uncertainty of 10 km. The plate interface based on that of Pardo and Suarez [1995] in the distance range where our NVT locations occur is between 40 and 53 km, suggesting that the depths of NVT sources could be consistent with them occurring on the plate interface. Yet we do not see a statistically significant dip in the distribution of NVT hypocenters, such that events near 200 km distance

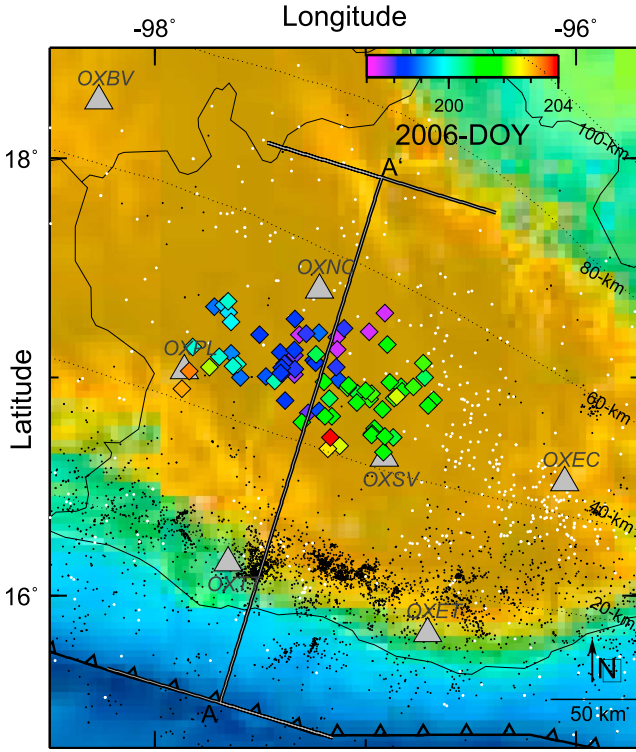


Figure 9. Map illustrating epicenters of NVT during the July 2006 episode (diamonds) and earthquakes during the first 9 months of recording (circles) [Jensen et al., 2008]. For NVT, colored shading indicates day of 2006 when it occurred. Earthquakes are shaded based on depth (black < 35 km, white > 35 km). Gray-black bars indicate the azimuth, distance, and along-strike width of cross-section A–A' shown in Figure 10. Layout is otherwise similar to Figure 1.

appear to be at least 10 km and as much 20 km above the plate interface. Two potential explanations for this discrepancy are (1) some NVT events occur within the upper plate, potentially reflecting fluid flow or a distributed shear zone [e.g., Kao et al., 2005], or (2) the dip of the plate interface is shallower in this region of Oaxaca. To consider the latter alternative, we have plotted a shallower interface model [Franco et al., 2005], which is based on a 2-D gravity and magnetic model as well as some intraslab seismicity. Compared to this model, nearly all NVT locations occur below the plate interface. A plate interface with a dip in between these two models would be the most consistent with our NVT locations, and appears to be consistent with examination of locally recorded seismicity [Jensen et al., 2008], but the fact remains that the plate interface and NVT locations are not currently well constrained enough in this region to propose NVT in Oaxaca is either restricted to the plate interface or prevalent above it.

5. Discussion

[28] Source locations from the July 2006 episode allow us to place NVT in the context of other recently identified features associated with the subduction of the Cocos plate. Of these features, the one that spatially correlates well with the locations of NVT is an area of high conductivity (Figure 10), identified from 2-D modeling of a profile of magnetotelluric measurements [Jödicke et al., 2006] (Figure 1). This area of high conductivity was interpreted as a location where slab derived fluids released by progressive metamorphic dehydration of the basaltic oceanic crust are stored within the overlying deep continental crust. The fact that our NVT locations occur precisely within this anomaly supports the notion that the physical process responsible for NVT is related to fluid release from the slab [e.g., Katsumata

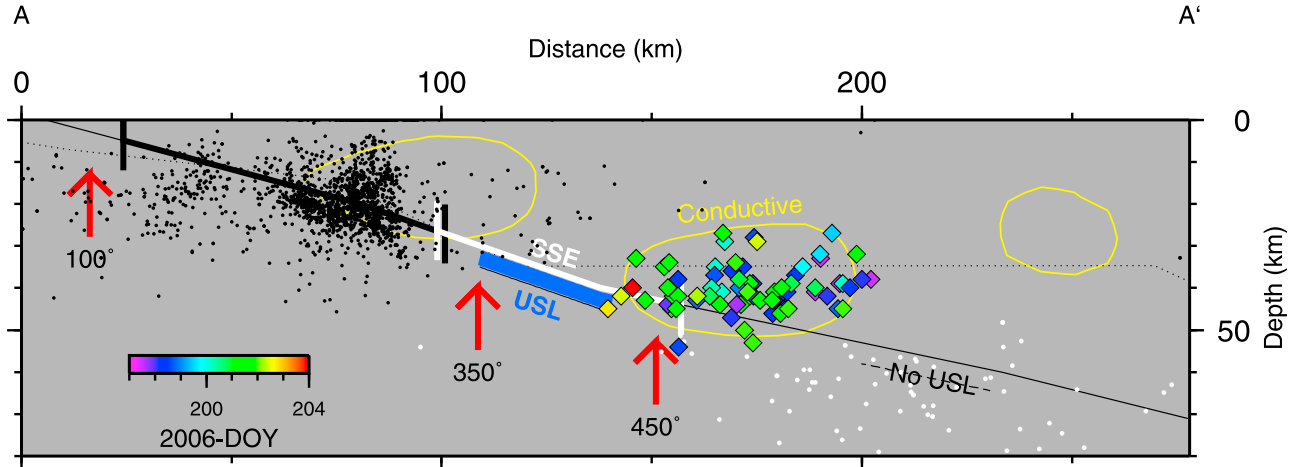


Figure 10. Cross-section showing NVT hypocenters during the July 2006 episode in the context of other recent observations. Location of cross-section and symbols for NVT and earthquake hypocenters are from Figure 9. Estimates of the plate interface are from Pardo and Suarez [1995] (solid line) and Franco et al. [2005] (dotted line). Extent of the 1978 megathrust earthquake (thick black line) and areas of >100 mm slip during two recent slow slip episodes (thick white line) are also shown. Red arrows denote temperature estimates on the plate interface [Currie et al., 2002]. Blue region is an ultra-slow velocity layer that is absent beyond 200 km distance. Yellow circles indicate high conductivity zones ($<30 \text{ ohm m}^{-1}$) after Jödicke et al. [2006].

and Kamaya, 2003; Schwartz and Rokosky, 2007]. The fact that tremor is not observed in either of the other two high conductivity zones suggests that other conditions necessary to produce tremor are not met in the other two regions, such as not being within a transitional zone of frictional behavior on the plate interface.

[29] GPS measurements of surface deformation from the Oaxaca segment have been modeled to characterize episodic slow slip along the subduction interface in this region as well [Correa-Mora et al., 2008; 2009]. One slow slip event finished in Oaxaca ~1 month before the time period we analyzed, and another slow slip event occurred during the time period we analyzed. When we compare the location of the two detected slow slip events to the hypocenters of the best recorded NVT episode, we find that slow slip occurs primarily trenchward and updip from the NVT (Figure 10). This supports the hypothesis that the Oaxaca region is behaving in a similar way to Nankai, where infrequent GPS-detected slow slip events occur updip from the locations of frequent NVT episodes. This pattern may be occurring in other areas of Mexico, as NVT locations based on a linear array in Guerrero suggest they also occur inland from GPS-detected slow slip [e.g., Domínguez et al., 2006; Larson et al., 2004; Payero et al., 2008].

[30] Since large GPS-detected slow slip events are displaced updip from NVT, they are not spatially correlated with a high conductivity zone in the overlying deep crust. Instead, they are associated with an observation of an ultra-slow velocity layer detected across southern Mexico with locally recorded converted phases and teleseismic underside reflections sampling the top of the subducting plate [Song et al., 2009] (Figure 10). This 3–5 km thick layer is ~40% slower than hydrated oceanic crust, suggesting it is fluid-saturated to form a high pore fluid pressure layer. High pore fluid pressures have been proposed in other settings to explain the existence of slow slip [e.g., Audet et al., 2009], as it would be expected to greatly reduce the effective normal stress on the plate interface, promoting episodic slow slip [e.g., Liu and Rice, 2005, 2007] and dynamic triggering of tremors [e.g., Rubinstein et al., 2007]. While these detailed velocity estimates of the subducting plate are sparse in Oaxaca, a measurement slightly inland from our NVT locations finds no evidence for the ultra-slow velocity layer, suggesting the high pore fluid pressures have dissipated beyond the region where high conductivity suggests slab fluids have infiltrated the overlying continental crust (Figure 10). It is not clear why there is no zone of high conductivity in the same location as the ultra-slow layer as both are commonly thought to indicate the prevalence of fluids. We can only speculate that perhaps the different geophysical signatures represent different characteristics of fluid within the rock and hope that this relates to the different seismological behaviors observed.

[31] The temperature along the plate interface has also been estimated in the vicinity of this cross-section via 2-D finite element modeling that incorporate parameters appropriate for the Oaxaca region [Currie et al., 2002]. We denote the locations of three isotherms to illustrate the thermally defined seismogenic “locked” zone (100°C–350°C) and transitional zone (350°C–450°C) [e.g., Hyndman and Wang, 1993] (Figure 10). As was noted by Currie et al. [2002], the thermally defined locked zone coincides well with the extent

of the previous megathrust rupture in 1978 defined by aftershock locations [e.g., Singh et al., 1980; Stewart et al., 1981]. Moreover, recent modeling of GPS measurements find that this same seismogenic region is strongly locked again and appears to have accumulated enough strain for a repeat earthquake [Correa-Mora et al., 2008]. We also find that earthquakes recorded locally during the same time period as our NVT analysis concentrate at the downdip end of the seismogenic zone [Jensen et al., 2008] (Figure 10). Intriguingly, the thermally defined transition zone corresponds almost entirely to the region of GPS-detected slow slip and high pore fluid pressures in Oaxaca, while NVT and corresponding high conductivities primarily occur further inland and presumably associated with higher temperatures on the interface. Whether the differing onsets of these zones of long-term slow slip and short-term NVT episodes are defined by temperature or other properties such as depth, petrology and fluid content will require compilation of a similar set of measurements in a variety of settings to isolate the different variables. In any case, the offset in slow slip and NVT suggest that the transition from locking to free slip may occur in more than one phase, progressing through different physical processes.

[32] Finally, we feel it is important to highlight that NVT locations are displaced 50–100 km inland from the downdip end of the seismogenic zone, as defined by a previous megathrust earthquake sequence as well as recent measurements of locking, microseismicity and temperatures. While NVT likely represents one aspect of the transition from locking to free slip, it is not necessarily adjacent to the locked zone. Thus, the updip edge of NVT locations alone should not be used to define the inland extent of rupture during future megathrust earthquakes.

6. Conclusion

[33] In this study, we established that NVT exists in the Oaxaca region based on spectrograms, appropriate phase moveouts, and waxing and waning of seismic energy on filtered day-long seismograms that were correlated across neighboring stations. Eighteen prominent NVT episodes that lasted upwards of a week occurred during the 15 months analyzed for this study, recurring as frequently as ~2–3 months. We analyze NVT envelope waveforms with a semiautomated process for identifying prominent energy bursts, and analyst-refined relative arrival times are inverted for source locations. NVT burst epicenters primarily occur between the 40–50 km contours for depth of the plate interface, except in eastern Oaxaca where they shift toward the 30 km contour as the slab steepens. Source locations of the best recorded and longest NVT episode show two main clusters in the western and central parts of our network offset in time by ~2 days. The median depth of NVT sources was 41 km, but uncertainty in the depths of the hypocenters and the plate interface make it premature to assess whether NVT is occurring on the interface or not. Nevertheless, NVT hypocenters correlate well with a high conductivity zone that was interpreted to be due to fluids released from the subducting plate. NVT is both more frequent and further inland than GPS-detected slow slip, which in turn is associated with a thin zone of ultra-slow velocity interpreted to represent high pore fluid pressure at the top of the sub-

ducting plate. The zone of slow slip corresponds to the thermally defined transition zone, with megathrust earthquakes, microseismicity, and locking occurring immediately updip from it. This leaves NVT primarily in a region further inland from the thermally defined transition zone, suggesting that transition from locking to free slip may occur in more than one phase.

[34] **Acknowledgments.** This project benefited from discussions with D. Boyarko, W.-P. Chen, K. Creager, H. DeShon, K. Jensen, W. McCausland, L. Powell, A. Song, and B. Unger. D. Boyarko, E. Brudzinski, S. Holtkamp, D. Kuentz, and S. Sit and the PASSCAL Instrument Center have contributed significantly to the deployment and maintenance of this seismic network. This research was supported by NSF-EAR 0510812 and Miami University's purchase of seismic instrumentation.

References

- Anderson, D. L. (1989), *Theory of the Earth*, 366 pp., Blackwell Sci., Boston, Mass.
- Astiz, L., and H. Kanamori (1984), An earthquake doublet in Ometepec, Guerrero, Mexico, *Phys. Earth Planet. Inter.*, **34**, 24–45, doi:10.1016/0031-9201(84)90082-7.
- Audet, P., M. G. Bostock, N. I. Christensen, and S. M. Peacock (2009), Seismic evidence for overpressured subducted oceanic crust and sealing of the megathrust, *Nature*, **457**, 76–78, doi:10.1038/nature07650.
- Beck, J. L., and J. F. Hall (1986), Factors contributing to the catastrophe in Mexico City during the earthquake of September 19, 1985, *Geophys. Res. Lett.*, **13**, 593–596, doi:10.1029/GL013i006p00593.
- Boyarko, D. C., and M. R. Brudzinski (2010), Spatial and temporal patterns of nonvolcanic tremor along the southern Cascadia subduction zone, *J. Geophys. Res.*, **115**, B00A22, doi:10.1029/2008JB006064.
- Brudzinski, M. R., and R. M. Allen (2007), Segmentation in episodic tremor and slip all along Cascadia, *Geology*, **35**, 907–910, doi:10.1130/G23740A.1.
- Brudzinski, M., E. Cabral-Cano, F. Correa-Mora, C. DeMets, and B. Márquez-Azúa (2007), Slow slip transients along the Oaxaca subduction segment from 1993 to 2007, *Geophys. J. Int.*, **171**, 523–538, doi:10.1111/j.1365-246X.2007.03542.x.
- Correa-Mora, F., C. DeMets, E. Cabral-Cano, B. Marquez-Azua, and O. Diaz-Molina (2008), Interplate coupling and transient slip along the subduction interface beneath Oaxaca, Mexico, *Geophys. J. Int.*, **175**, 269–290, doi:10.1111/j.1365-246X.2008.03910.x.
- Correa-Mora, F., C. DeMets, E. Cabral-Cano, O. Diaz-Molina, and B. Marquez-Azúa (2009), Transient deformation in southern Mexico in 2006 and 2007: Evidence for distinct deep-slip patches beneath Guerrero and Oaxaca, *Geochem. Geophys. Geosyst.*, **10**, Q02S12, doi:10.1029/2008GC002211.
- Courboulex, F., M. A. Santoyo, J. F. Pacheco, and S. K. Singh (1997), The 14 September 1995 ($M = 7.3$) Copala, Mexico, earthquake: A source study using teleseismic, regional, and local data, *Bull. Seismol. Soc. Am.*, **87**, 999–1010.
- Currie, C. A., R. D. Hyndman, K. Wang, and V. Kostoglodov (2002), Thermal models of the Mexico subduction zone: Implications for the megathrust seismogenic zone, *J. Geophys. Res.*, **107**(B12), 2370, doi:10.1029/2001JB000886.
- Dominguez, J., G. Suárez, D. Comte, and L. Quintanar (2006), Seismic velocity structure of the Guerrero gap, Mexico, *Geofis. Int.*, **45**, 129–139.
- Dragert, H., K. L. Wang, and T. S. James (2001), A silent slip event on the deeper Cascadia subduction interface, *Science*, **292**, 1525–1528, doi:10.1126/science.1060152.
- Efron, B. (1979), Bootstrap methods: Another look at the jackknife, *Ann. Stat.*, **7**, 1–26, doi:10.1214/aos/1176344552.
- Franco, S. I., V. Kostoglodov, K. M. Larson, V. C. Manea, M. Manea, and J. A. Santiago (2005), Propagation of the 2001–2002 silent earthquake and interplate coupling in the Oaxaca subduction zone, Mexico, *Earth Planets Space*, **57**, 973–985.
- Hermann, R.-B. (2004), Computer programs in seismology, version 3.30-GSAC, Saint Louis Univ., Saint Louis, Mo.
- Hirn, A., and M. Laigle (2004), Geophysics: Silent heralds of megathrust earthquakes?, *Science*, **305**, 1917–1918, doi:10.1126/science.1101152.
- Hirose, H., and K. Obara (2005), Repeating short- and long-term slow slip events with deep tremor activity around the Bungo channel region, southwest Japan, *Earth Planets Space*, **57**, 961–972.
- Hirose, H., K. Hirahara, F. Kimata, N. Fujii, and S. Miyazaki (1999), A slow thrust slip event following the two 1996 Hyuganada earthquakes beneath the Bungo Channel, southwest Japan, *Geophys. Res. Lett.*, **26**, 3237–3240, doi:10.1029/1999GL010999.
- Hyndman, R. D., and K. Wang (1993), Thermal constraints on the zone of major thrust earthquake failure: The Cascadia subduction zone, *J. Geophys. Res.*, **98**, 2039–2060, doi:10.1029/92JB02279.
- Ide, S., G. C. Beroza, D. R. Shelly, and T. Uchide (2007a), A scaling law for slow earthquakes, *Nature*, **447**, 76–79, doi:10.1038/nature05780.
- Ide, S., D. R. Shelly, and G. C. Beroza (2007b), Mechanism of deep low frequency earthquakes: Further evidence that deep nonvolcanic tremor is generated by shear slip on the plate interface, *Geophys. Res. Lett.*, **34**, L03308, doi:10.1029/2006GL028890.
- Jensen, K., T. Carey, M. Brudzinski, H. DeShon, E. Cabral-Cano, A. Arciniega-Ceballos, O. Diaz-Molina, and C. DeMets (2008), Seismicity of the Oaxaca segment of the Middle American subduction zone, *Eos Trans. AGU*, **89**(53), Fall Meet. Suppl., Abstract T13F-08.
- Jödicke, H., A. Jording, L. Ferrari, J. Arzate, K. Mezger, and L. Rupke (2006), Fluid release from the subducted Cocos plate and partial melting of the crust deduced from magnetotelluric studies in southern Mexico: Implications for the generation of volcanism and subduction dynamics, *J. Geophys. Res.*, **111**, B08102, doi:10.1029/2005JB003739.
- Kao, H., and S. J. Shan (2004), The Source-Scanning Algorithm: Mapping the distribution of seismic sources in time and space, *Geophys. J. Int.*, **157**, 589–594, doi:10.1111/j.1365-246X.2004.02276.x.
- Kao, H., S. J. Shan, H. Dragert, G. Rogers, J. F. Cassidy, and K. Ramachandran (2005), A wide depth distribution of seismic tremors along the northern Cascadia margin, *Nature*, **436**, 841–844, doi:10.1038/nature03903.
- Kao, H., S. J. Shan, H. Dragert, G. Rogers, J. F. Cassidy, K. L. Wang, T. S. James, and K. Ramachandran (2006), Spatial-temporal patterns of seismic tremors in northern Cascadia, *J. Geophys. Res.*, **111**, B03309, doi:10.1029/2005JB003727.
- Kao, H., S.-J. Shan, H. Dragert, and G. Rogers (2009), Northern Cascadia episodic tremor and slip: A decade of tremor observations from 1997 to 2007, *J. Geophys. Res.*, **114**, B00A12, doi:10.1029/2008JB006046.
- Katsumata, A., and N. Kamaya (2003), Low-frequency continuous tremor around the Moho discontinuity away from volcanoes in the southwest Japan, *Geophys. Res. Lett.*, **30**(1), 1020, doi:10.1029/2002GL015981.
- Kodaira, S., T. Iidaka, A. Kato, J. O. Park, T. Iwasaki, and Y. Kaneda (2004), High pore fluid pressure may cause silent slip in the Nankai Trough, *Science*, **304**, 1295–1298, doi:10.1126/science.1096535.
- Kostoglodov, V., and L. Ponce (1994), Relationship between subduction and seismicity in the Mexican part of the Middle America Trench, *J. Geophys. Res.*, **99**, 729–742, doi:10.1029/93JB01556.
- Larson, K. M., A. R. Lowry, V. Kostoglodov, W. Hutton, O. Sánchez, K. Hudnut, and G. Suárez (2004), Crustal deformation measurements in Guerrero, Mexico, *J. Geophys. Res.*, **109**, B04409, doi:10.1029/2003JB002843.
- Liu, Y., and J. R. Rice (2005), Aseismic slip transients emerge spontaneously in three-dimensional rate and state modeling of subduction earthquake sequences, *J. Geophys. Res.*, **110**, B08307, doi:10.1029/2004JB003424.
- Liu, Y., and J. R. Rice (2007), Spontaneous and triggered aseismic deformation transients in a subduction fault model, *J. Geophys. Res.*, **112**, B09404, doi:10.1029/2007JB004930.
- Lowry, A. R., K. M. Larson, V. Kostoglodov, and R. Bilham (2001), Transient fault slip in Guerrero, southern Mexico, *Geophys. Res. Lett.*, **28**, 3753–3756, doi:10.1029/2001GL013238.
- Márquez-Azúa, B., and C. DeMets (2003), Crustal velocity field of Mexico from continuous GPS measurements, 1993 to June 2001: Implications for the neotectonics of Mexico, *J. Geophys. Res.*, **108**(B9), 2450, doi:10.1029/2002JB002241.
- Mazzotti, S., and J. Adams (2004), Variability of near-term probability for the next great earthquake on the Cascadia subduction zone, *Bull. Seismol. Soc. Am.*, **94**, 1954–1959, doi:10.1785/012004032.
- Nadeau, R. M., and D. Dolenc (2005), Nonvolcanic tremors deep beneath the San Andreas Fault, *Science*, **307**, 389, doi:10.1126/science.1107142.
- Obara, K. (2002), Nonvolcanic deep tremor associated with subduction in southwest Japan, *Science*, **296**, 1679–1681, doi:10.1126/science.1070378.
- Obara, K., and H. Hirose (2006), Non-volcanic deep low-frequency tremors accompanying slow slips in the southwest Japan subduction zone, *Tectonophysics*, **417**, 33–51, doi:10.1016/j.tecto.2005.04.013.
- Obara, K., H. Hirose, F. Yamamizu, and K. Kasahara (2004), Episodic slow slip events accompanied by nonvolcanic tremors in southwest Japan subduction zone, *Geophys. Res. Lett.*, **31**, L23602, doi:10.1029/2004GL020848.
- Obara, K., K. Kasahara, S. Hori, and Y. Okada (2005), A densely distributed high-sensitivity seismograph network in Japan: Hi-net by National

- Research Institute for Earth Science and Disaster Prevention, *Rev. Sci. Instrum.*, 76, 021301, doi:10.1063/1.1854197.
- Okada, Y., K. Kasahara, S. Hori, K. Obara, S. Sekiguchi, H. Fujiwara, and A. Yamamoto (2004), Recent progress of seismic observation networks in Japan: Hi-net, F-net, K-NET and KiK-net, *Earth Planets Space*, 56, XV–XXVIII.
- Ozawa, S., M. Murakami, M. Kaidzu, T. Tada, T. Sagiya, Y. Hatanaka, H. Yarai, and T. Nishimura (2002), Detection and monitoring of ongoing aseismic slip in the Tokai region, central Japan, *Science*, 298, 1009–1012, doi:10.1126/science.1076780.
- Pardo, M., and G. Suarez (1995), Shape of the subducted Rivera and Cocos plates in southern Mexico: Seismic and tectonic implications, *J. Geophys. Res.*, 100, 12,357–12,373, doi:10.1029/95JB00919.
- Payero, J. S., V. Kostoglodov, N. Shapiro, T. Mikumo, A. Iglesias, X. Perez-Campos, and R. W. Clayton (2008), Nonvolcanic tremor observed in the Mexican subduction zone, *Geophys. Res. Lett.*, 35, L07305, doi:10.1029/2007GL032877.
- Rogers, G., and H. Dragert (2003), Episodic tremor and slip on the Cascadia subduction zone: The chatter of silent slip, *Science*, 300, 1942–1943, doi:10.1126/science.1084783.
- Rubinstein, J. L., J. E. Vidale, J. Gomberg, P. Bodin, K. C. Creager, and S. D. Malone (2007), Non-volcanic tremor driven by large transient shear stresses, *Nature*, 448, 579–582, doi:10.1038/nature06017.
- Scholz, C. H. (1990), Mechanics of Earthquakes and Faulting, 439 pp., Cambridge Univ. Press, Cambridge, U. K.
- Schwartz, S. Y., and J. M. Rokosky (2007), Slow slip events and seismic tremor at circum-Pacific subduction zones, *Rev. Geophys.*, 45, RG3004, doi:10.1029/2006RG000208.
- Shelly, D. R., G. C. Beroza, S. Ide, and S. Nakamura (2006), Low-frequency earthquakes in Shikoku, Japan, and their relationship to episodic tremor and slip, *Nature*, 442, 188–191, doi:10.1038/nature04931.
- Shelly, D. R., G. C. Beroza, and S. Ide (2007), Complex evolution of transient slip derived from precise tremor locations in western Shikoku, Japan, *Geochem. Geophys. Geosyst.*, 8, Q10014, doi:10.1029/2007GC001640.
- Singh, S. K., J. Havskov, K. McNally, L. Ponce, T. Hearn, and M. Vassiliou (1980), The Oaxaca, Mexico, earthquake of 29 November 1978: A preliminary report on aftershocks, *Science*, 207, 1211–1213, doi:10.1126/science.207.4436.1211.
- Singh, S. K., J. Pacheco, E. Courboulex, and D. A. Novelo (1997), Source parameters of the Pinotepa Nacional, Mexico, earthquake of 27 March, 1996 (Mw = 5.4) estimated from near-field recordings of a single station, *J. Seismol.*, 1, 39–45, doi:10.1023/A:1009741712512.
- Song, T.-R. A., D. Helmberger, M. R. Brudzinski, R. W. Clayton, P. Davis, X. Pérez-Campos, and S. K. Singh (2009), Subducting slab ultra-slow velocity layer coincident with silent earthquakes in southern Mexico, *Science*, 324, 502–506, doi:10.1126/science.1167595.
- Stern, R. J. (2002), Subduction zones, *Rev. Geophys.*, 40(4), 1012, doi:10.1029/2001RG000108.
- Stewart, G. S., E. P. Chael, and K. C. McNally (1981), The November 29, 1978, Oaxaca, Mexico, earthquake: A large simple event, *J. Geophys. Res.*, 86, 5053–5060, doi:10.1029/JB086iB06p05053.
- Szeliga, W., T. I. Melbourne, M. M. Miller, and V. M. Santillan (2004), Southern Cascadia episodic slow earthquakes, *Geophys. Res. Lett.*, 31, L16602, doi:10.1029/2004GL020824.
- Tajima, F., and K. C. McNally (1983), Seismic rupture patterns in Oaxaca, Mexico, *J. Geophys. Res.*, 88, 4263–4275, doi:10.1029/JB088iB05p04263.
- Valdes, C. M., W. D. Mooney, S. K. Singh, R. P. Meyer, C. Lomnitz, J. H. Luetgert, C. E. Helsley, B. T. R. Lewis, and M. Mena (1986), Crustal structure of Oaxaca, Mexico, from seismic refraction measurements, *Bull. Seismol. Soc. Am.*, 76, 547–563.
- Wech, A. G., and K. C. Creager (2008), Automated detection and location of Cascadia tremor, *Geophys. Res. Lett.*, 35, L20302, doi:10.1029/2008GL035458.
-
- A. Arciniega-Ceballos, Departamento de Vulcanología, Instituto de Geofísica, Universidad Nacional Autónoma de México, Ciudad Universitaria del Coyoacán, México D.F., CP 04510, México.
- M. R. Brudzinski, H. R. Hinojosa-Prieto, and K. M. Schlanser, Department of Geology, Miami University of Ohio, 103 Shideler Hall, Oxford, OH 45056, USA. (brudzimr@muohio.edu)
- E. Cabral-Cano and O. Diaz-Molina, Departamento de Geomagnetismo y Exploración, Instituto de Geofísica, Universidad Nacional Autónoma de México, Ciudad Universitaria, México D.F., CP 04510, México.
- C. DeMets, Department of Geology and Geophysics, University of Wisconsin-Madison, 1215 West Dayton St., Madison, WI 53706, USA.